EasyChair Preprint

№ 9393

A Real-Time Flood Forecasting Hybrid Machine Learning Hydrological Model for Krong H'Nang Hydropower Reservoir

Phuoc Sinh Nguyen, Truong Huy Nguyen and The Hung Nguyen

November 30, 2022

A real-time flood forecasting hybrid machine learning hydrological model for Krong H'nang hydropower reservoir

Phuoc Sinh Nguyen[1,2*], Truong Huy Nguyen[1,3], The Hung Nguyen[2]

[1] Faculty of Water Resources Engineering, University of Science and Technology-The University of Da Nang, 50000, Vietnam.
[2] Song Ba JSC, 573 Nui Thanh, Hai Chau, Da Nang, 50000, Vietnam.
[3] Department of Civil Engineering, McGill University, 817 Sherbrooke Street West, Montreal, Quebec H3A 2K6, Canada

*phuocsinhbk@gmail.com; huy.nguyen5@mail.mcgill.ca; ngthung@dut.udn.vn

Abstract. Flood forecasting is critical for mitigating flood damage and ensuring a safe operation of hydroelectric power plants and reservoirs. In this paper, the authors present a hybrid machine learning hydrological model to enhance the accuracy of a real-time flood forecasting. This model is developed based on the combination of the HEC-HMS hydrological model and an Encoder-Decoder-Long Short-Term Memory network. The proposed hybrid model has been applied to the Krong H'nang hydropower reservoir. The observed data from 33 floods monitored between 2016 and 2021 are used to calibrate, validate, and test the hybrid model. Results show that the HEC-HMS-ANN hybrid model significantly improves the forecast quality, especially for long forecasting time steps. The KGE efficiency index, for example, increased from $\Delta KGE = 16\%$ at time $t + 1$ to $\Delta KGE = 69\%$ at time $t + 6$ hours, similar to other indicators (such as peak error and volume error). The computer program developed for this study is being used at the KrongHnang hydropower to aid in reservoir planning, flood control, and water resource efficiency.

Keywords. Hydrological hybrid model, HEC-HMS, machine learning, KrongH'nang, real-time flood forecasting.

1. Introduction

In recent years, extreme weather patterns such as rainfall and floods have appeared with increasing frequency and intensity, exceeding historical values. Some studies have shown that under the impact of climate change, extreme rainfall events may occur more frequently, increasing the severity of flooding [1,2]. Flood forecasting and warning information are thus critical to relevant authorities and departments in planning to prevent, respond to, and mitigate the harmful effects of floods, as well as evacuate people from flood-prone areas. Furthermore, this data assists state management agencies, such as irrigation and hydropower plant operators, in controlling floods to ensure safety for the structure and downstream areas [3,4].

There are different methods and approaches, ranging from simple to complex, for modeling the rainfall-runoff relationship. These methods can be divided into two types: physically-based models and data-driven models. Which method should be selected is determined by the amount of data available in each case study [5]. Several hydrological physical-base models that have been widely studied and applied in practice, such as MIKE-NAM, SWAT, HEC-HMS, and so on, have shown the feasibility of

simulating and forecasting the rainfall-runoff scenario [6–8]. However, these models often require a variety of data types (e.g., topographic, geomorphological, meteorological, and hydrological data) and in-depth modeling expertise to establish relevant databases on the rainfall-runoff characteristics of each study basin. It also takes a long time to adjust the parameters and evaluate the model, making it difficult to respond quickly to flood events that fluctuate [9,10].

In the meanwhile, the goal of data-driven models is to establish correlations between precipitation and discharge from observed data without taking related physical processes into account. Common models in this group can be mentioned as linear regression models, nonlinear regression models, autoregressive integrated moving averages (ARIMA), artificial neural networks (ANN), adaptive neuro-fuzzy inference systems (ANFIS), and support vector machines (SVM). In the models mentioned above, the artificial neural network model has been widely applied to many hydrological problems. A number of previous studies have demonstrated that ANN models outperform other classical techniques in terms of their ability to simulate complex nonlinear processes of input and output variables. The ANN models can be trained to capture the nonlinear rainfall-runoff relationship and predict runoff quantitatively without prior knowledge of basin characteristics [11,12]. The limitation of this approach is that the user cannot access the internal logic (black box model), and it does not show the physical characteristics of rainfall-runoff, topographic changes, and surface buffer factors on the catchment [13].

The hydrological hybrid model was created to combine the advantages of both types of models. Many authors have investigated the interaction of data-driven models with physically-based models such as SWMM [14], SWAT [15], and HEC-RAS [16] to forecast floods, and urban flooding and shown the superiority of the hybrid model. However, the application of ANN to hydrological problems in Vietnam is still in its early stages, specific applied research is required to demonstrate both the effectiveness and limitations that may be encountered when using it for flood forecasting decision support on reservoir operation.

In this study, the hybrid machine learning hydrological model, which combines the HEC-HMS and ANN model, was developed and tested for the Krong H'nang hydropower reservoir located in the Dak Lak province. First, the HEC-HMS physical-base hydrology model will be built to simulate the rainfall-runoff process in the basin. The output from the HEC-HMS will continue to be the input variable for the ANN model using the Encoder-Decoder-Long Short Term Memory (LSTM) architecture [12,17]. Data from 33 floods from 2016 to 2021 is divided into three data sets for training, validation, and testing in the following proportions 70:15:15. The results of the hybrid model will be evaluated in detail, considering the degree of improvement in flood forecasting quality at time steps compared to the HEC-HMS model.

2. Study Area and Data Used

Krong H'nang is one of the major hydroelectric projects in the Ba River basin, one of the largest river catchment in the South-Central region of Vietnam. The earth dam was built on the Ea KrongH’nang River, which has a length of 1,068 meters and is located on National Highway 29, about 80 kilometers northeast of Buon Ma Thuot (Dak Lak province). The basin has an area of 1,168 km^2 with the terrain divided by the Truong Son range and the plateau, forming two distinct topographical regions (**Figure 1**). The upstream area with a topographic elevation above 500 m is the basalt red soil plateau, planted with industrial crops and influenced by the southwest monsoon during the rainy season from May to November. While the downstream area is a plain of rice and cash crops with elevations from 240 to 500 m, interspersed with mountain ranges with peaks of up to 1,200 m, forming valleys with steep slopes of 8–15% during the rainy season from September to December and is strongly influenced by the northeast monsoon, tropical depressions, and storms in the East Sea [18].

Data for the period from September 2016 to December 2021 includes rainfall data from 15 gauges, measurement inflow data, and the HEC-HMS simulation output data at 33 floods (15-minute intervals), which is used as input data for the hybrid model. Evaporation losses from the reservoir are normally small during the flood season and are ignored in the model. The MinmaxScaler function (1) normalizes the input data to the range [0, 1] to improve the ANN model's training speed and learning efficiency.

$$x_{scaler} = \frac{x - x_{min}}{x_{max} - x_{min}} \quad (1)$$

Where x is the raw value, x_{caler} is the value after normalization.

As shown in **Figure 2**, the entire dataset will be divided into subsets with the respective proportions of 70% for model training, 15% for calibration, and 15% for testing.

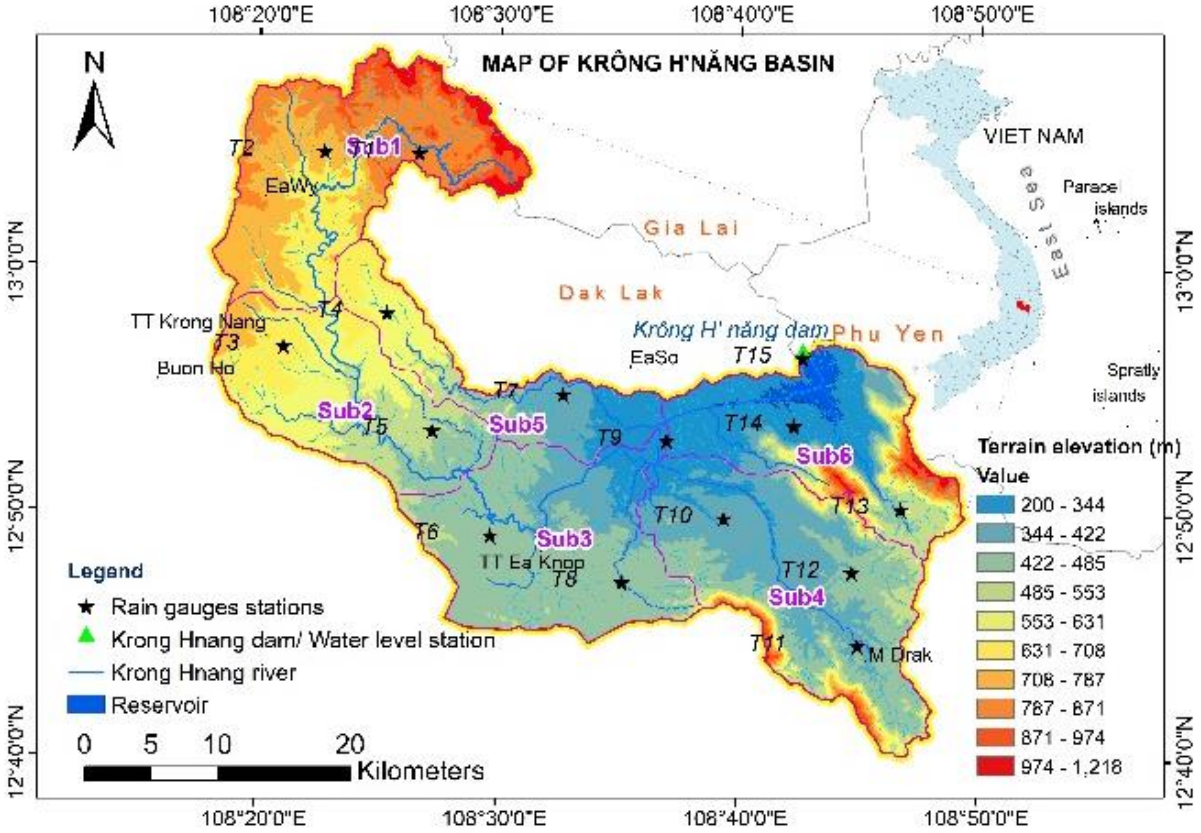

Figure 1. Map of Krong H'nang river basin. The main basin is divided into six sub-basins (Sub1 to Sub6). Color indicates the elevation from low (blue color) to high (red color). The star markers show the locations of 15 automatic rain gauges (T1 to T15). The green triangle represents the location of Krong H'nangdam and the automatic water lever gauges.

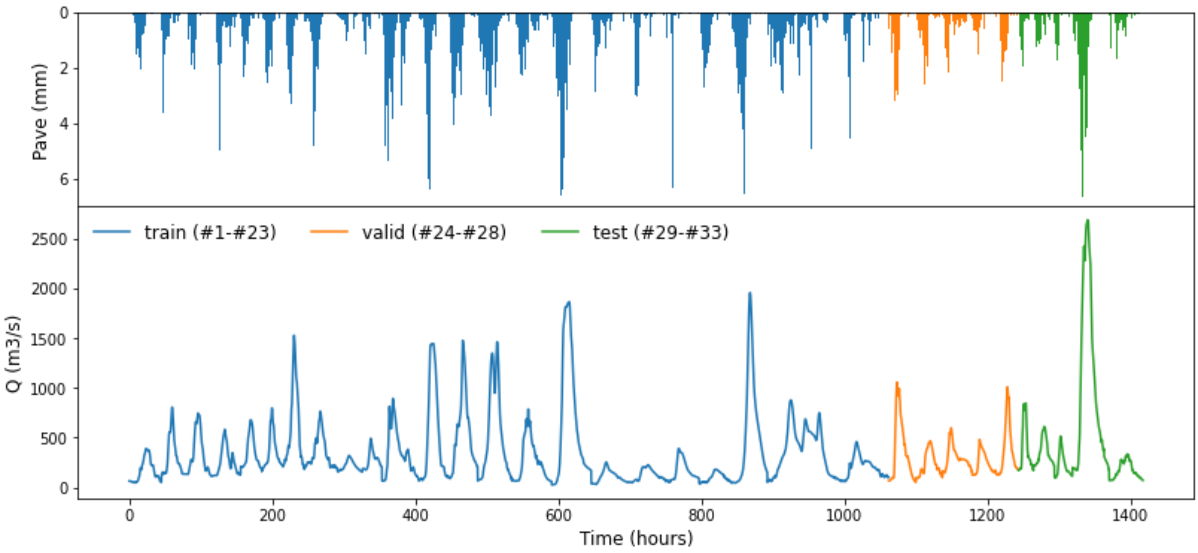

Figure 2. Data from 33 flood events ranging from 2016 to 2021 at Krong H'nang hydropower reservoir (data between floods is not displayed). The dataset was divided for training, calibration (valid), and testing at the ratio of 70:15:15.

3. Methodology

3.1. Model structure and descriptions

The HEC-HMS-ANN hybrid model structure is illustrated in **Figure 3** with an input layer consisting of 15 stations of rainfall data (X_1, X_2,…, X_{15}), measured discharge (Q_{obs}) ranging from the last 8 hours ($t-8$) to now (t = 0), and forecasted data from the HEC-HMS model (Q_{hms}) ahead to $t+6$ hours. The hidden layer consists of k layer with n neural in each layer. The output layer is the prediction of the reservoir's inflow Q_{pre}.

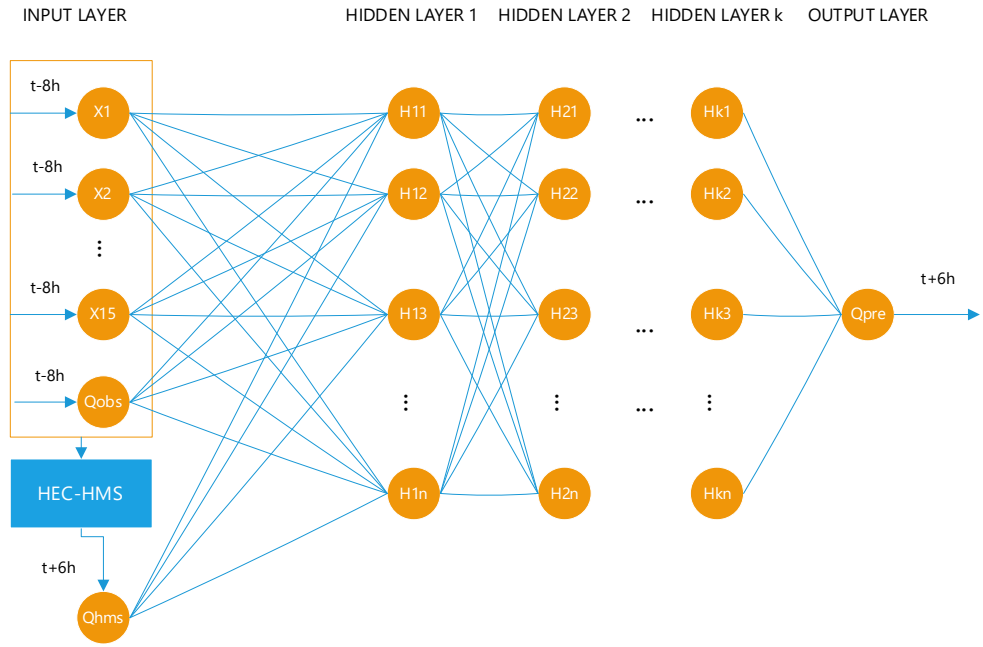

Figure 3. The hybrid hydrological model structure, which combines the HEC-HMS and ANN model.

The size of the input data series for the ANN model is critical and has a large impact on the model results, but there is currently no specific theoretical formula for this. However, we can rely on the correlation analysis between flood discharge and its delay or with the delay of another time series (such as precipitation) through the cross-correlation function (CCF) defined by expression (2) to make a reasonable decision.

$$CCF_{xy}^{k} = \frac{CVF_{xy}^{k}}{\sqrt{\sigma_x \sigma_y.}} \quad (2)$$

Where k is the number of lag time; σ_x and σ_y are the standard deviation of x and y; CVF_{xy}^{k} iss the cross-covariance function of x and y, determined by the expression (3).

$$CVF_{xy}^{k} = \frac{1}{N_t - 1} \sum_{t=1}^{N_t - k} (y_t - \bar{y}) . (x_{t+k} - \bar{x}) \quad (3)$$

Whe t is time steps; $\bar{x}$ and $\bar{y}$ are mean of x and y, N_t is number of data point of time series.

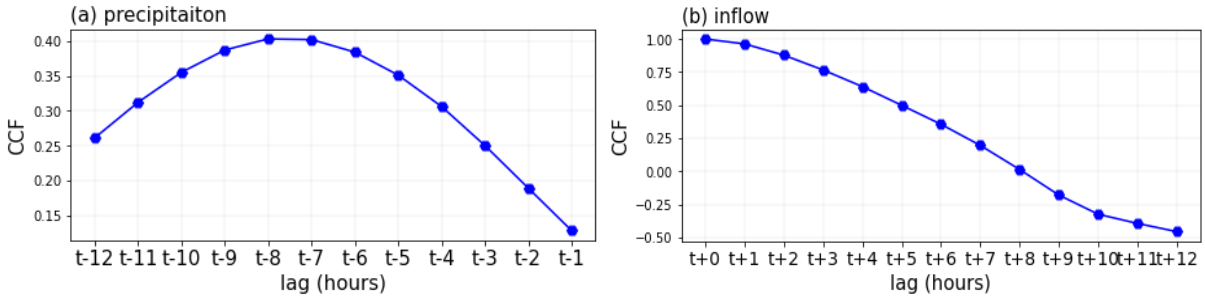

Figure 4. The cross-correlation function (CCF) bettwen reservoir's inflow with (a) average precipitation, and (b) reservoir's inflow at lag-time steps.

Based on the results of cross-correlation analysis of rainfall and runoff data series at lag-time steps shown in **Figure 4**, the sequence length has a high correlation with the target series (forecast flow) selected from t - 8 hours to t + 6 hours (see **Table 1**).

Table 1. Input and output data for the HEC-HMS-ANN hybrid model at different time steps.

Data	Time steps (h)										
	t-8	t-7	…	t-2	t-1	**t**	t+1	t+2	…	t+5	t+6
X_1, X_2,..,X_{15} (mm)	✓	✓	✓	✓	✓	✓					
X_{pre} (mm)											
Q_{obs} (m^3/s)	✓	✓	✓	✓	✓	✓					
Q_{hms} (m^3/s)	✓	✓	✓	✓	✓	✓	✓	✓	✓	✓	✓
Q_{pre} (m^3/s)						✓	✓	✓	✓	✓	✓

(Notes: The symbol ✓ represents the avaiable data used, the remaining cells have no data.)

3.2. The hydrological HEC-HMS model

The Hydrologic Engineering Center- Hydrologic Modeling System (HEC-HMS) was developed by the Hydrologic Engineering Center - U.S. Army (USACE) [19]. **Figure 5** illustrates the HEC-HMS process that simulates the hydrological processes of a watershed from precipitation to watershed discharge

through physical components and cycles: precipitation, evaporation, infiltration, overland flow, base flow, and stream channel.

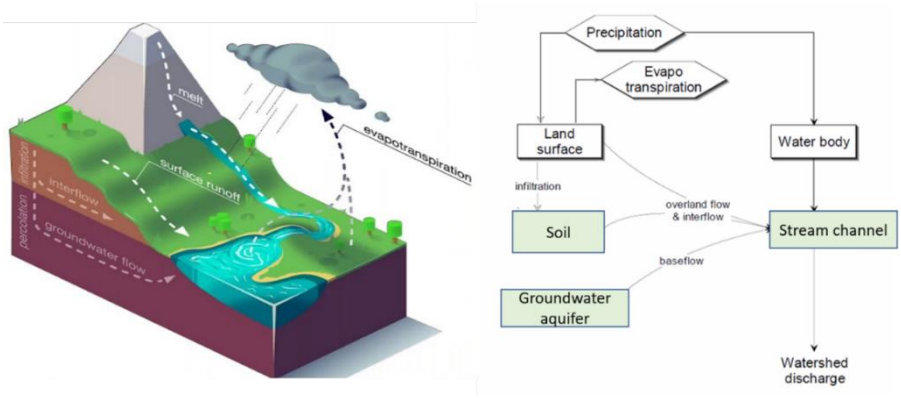

Figure 5. Illustrate the natural rainfall-runoff process and the flow diagram from the rainfall in the hydrological HEC-HMS model [20].

3.3. Encoder-Decoder-Long Short Term Memory Network

The Long Short-Term Memory Network (LSTM) is a special neural network architecture, designed by Hochreiter and Schmidhuber (1997) to overcome the weakness of traditional regressive neural networks by virtue of its ability to learn information in the long term. For the rainfall-runoff problem, this is extremely meaningful because it is possible to use rainfall-runoff data from the past for a long time to forecast the flow in accordance with the characteristics of water storage and the natural lag time in the basin.

The structure of the LSTM consists of four hidden layers (3 sigmoids and 1 tanh) that interact in a special way (see **Figure *6***). The idea behind LSTM is that the cell state, which is a kind of straight-line conveyor belt, performs mathematical operations (vector multiplication, addition) to aid in the stable transmission of information across the entire network. The transformation, transmission, and storage of information in the LSTM network through the steps described in expressions from (4) to (9).

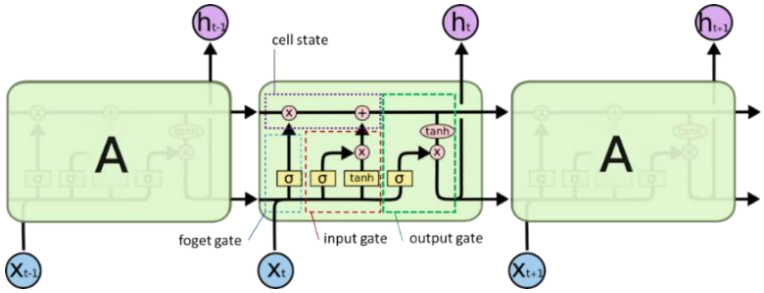

Figure 6. The LSTM network's iterative architecture module that contains four hidden layers (3 sigmoid and 1 tanh) that interact with one another [21].

$$f_t = \sigma\left(W_f . x_t + U_f h_{t-1} + b_f\right) \quad (4)$$

$$\widetilde{C}_t = tanh(W_{\tilde{c}} . x_t + U_{\tilde{c}} h_{t-1} + b_{\tilde{c}}) \quad (5)$$

$$i_t = \sigma(W_i . x_t + U_i h_{t-1} + b_i) \quad (6)$$

$$C_t = f_t * C_{t-1} + i_t * \widetilde{C}_t \quad (7)$$

$$o_t = \sigma(W_o x_t + U_o h_{t-1} + b_o) \quad (8)$$

$$h_t = o_t * tanh(C_t) \quad (9)$$

Where i_t , f_t, o_t are the input gate, the forget gate, and the output gate, respectively; W_i, W_f , and W_o represent the weights connecting input, forget, and output gates with the input, respectively; U_i , U_f,

and U_o denote the weights from input, forget, and output gates to the hidden states, respectively; b_i, b_f, and b_o are input, forget, and output gate bias vectors, respectively; $\widetilde{C_t}$ is the cell input; C_t is the current cell state; ; h_t refers to current hidden state; $*$ is element-wise multiplication; σ is the logistic sigmoidal function and $tanh$ is the hyperbolic tangent function.

An encoder and a decoder combined with the LSTM network layers form the Encoder-Decoder LSTM architecture (**Figure 7**), which is effectively used with problems involving time-sequential data series of length input and output strings are different and include many input and output variables.

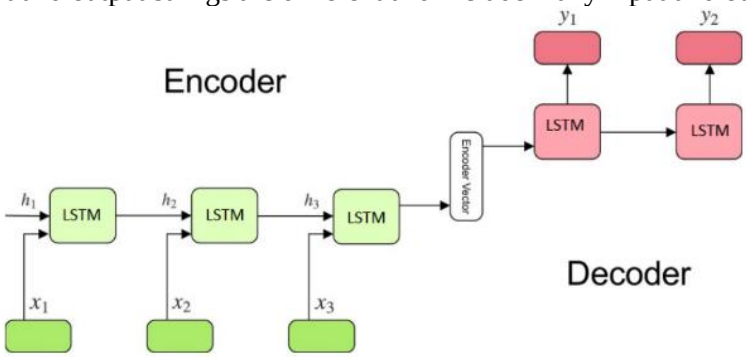

Figure 7. Architecture of the Encoder-Decoder-LSTM network (src: medium.com)

3.4. Model performance assessment

To evaluate the performance of the model in capturing the real hydrologic system, several commonly used numerical indicators are selected. These include the percent error in peak discharge, the percent error in discharge volume, the Kling-Gupta efficiency (KGE, dimensionless). These equations are as follows:

- Relative peak error (%):

$$\text{Peak error} = \frac{\mathrm{Q}^{\mathrm{p}}_{\mathrm{sim}} - \mathrm{Q}^{\mathrm{p}}_{\mathrm{obs}}}{\mathrm{Q}^{\mathrm{p}}_{\mathrm{obs}}} \tag{10}$$

- Relative volume error (%):

$$\text{Vol error} = 100.\frac{\mathrm{V}_{\mathrm{sim}} - \mathrm{V}_{\mathrm{obs}}}{\mathrm{V}_{\mathrm{obs}}} \tag{11}$$

- Kling-Gupta Efficiency (KGE):

$$\mathrm{KGE} = 1 - \sqrt{(R-1)^2 + (\alpha-1)^2 + (\beta-1)^2} \tag{12}$$

Where:

$$\mathrm{R} = \frac{\sum_{\mathrm{i=1}}^{\mathrm{n}} (\mathrm{Q}^{\mathrm{i}}_{\mathrm{obs}} - \overline{\mathrm{Q}_{\mathrm{obs}}}).(\mathrm{Q}^{\mathrm{i}}_{\mathrm{sim}} - \overline{\mathrm{Q}_{\mathrm{sim}}})}{\sqrt{\sum_{\mathrm{i=1}}^{\mathrm{n}} (\mathrm{Q}^{\mathrm{i}}_{\mathrm{obs}} - \overline{\mathrm{Q}_{\mathrm{obs}}})^2}\sqrt{\sum_{\mathrm{i=1}}^{\mathrm{n}} (\mathrm{Q}^{\mathrm{i}}_{\mathrm{sim}} - \overline{\mathrm{Q}_{\mathrm{sim}}})^2}} \tag{13}$$

$$\alpha = \frac{\sigma_{sim}}{\sigma_{obs}} \tag{14}$$

$$\beta = \frac{\mu_{sim}}{\mu_{obs}} \tag{15}$$

Where n is the total number of data points, Q (m^3/s) denotes discharge and V (m^3) is volume values at control points, σ is the standard deviation and $\overline{Q}$ is the mean of time-series data. Subscript sim and obs denote simulated and observed time-series data, respectively.

The proportion of improvement in the hybrid model's good level compared to the single HEC-HMS model is calculated by increasing or decreasing the index values (%) according to expression (16).

$$\Delta_M = \frac{(M_1 - M_i) - (M_2 - M_i)}{(M_1 - M_i)} . 100\ (\%) \qquad (16)$$

Where Δ_M is the degree of improvement in the M metric (KGE, Vol error, Peak error); M_1, M_2 are the evaluation indicators of the HEC-HMS model and the hybrid model, respectively; M_i is the *ideal* value of indicators: $\text{KGE} = 1;\ \text{Vol error} = 0;\ \text{Peak error} = 0$.

4. Results and Discussion

4.1. The HEC-HMS model

The Krong H'ang basin, with an area of 1,168 km^2, is divided into 6 sub-basins (from Sub1 to Sub6). The main river from the outlet of sub-basin Sub1 through to Krong H'nang reservoir is divided into 4 river sections (from Reach1 to Reach4) based on the topographic and hydrological characteristics of the basin. The components of the sub-basins and reaches are connected through junctions. The Krong H'nang catchment is established on the HEC-HMS model shown in **Figure 8**. The sub-basins area and the reach's length are measurable physical parameters, detailed in **Table 2**. There are 15 automatic rain gauges in the Krong H'nang basin. The rainfall data from the stations is calculated and converted to the average rainfall of the sub-basins according to the Thiessen polygon method. The optimal model parameters are automatically detected by the SCE-UA method [22]. The results of running the HEC-HMS model for 33 floods in a 15-minute time step ($Qhms$) are stored in the database for convenience in training the ANN model [23].

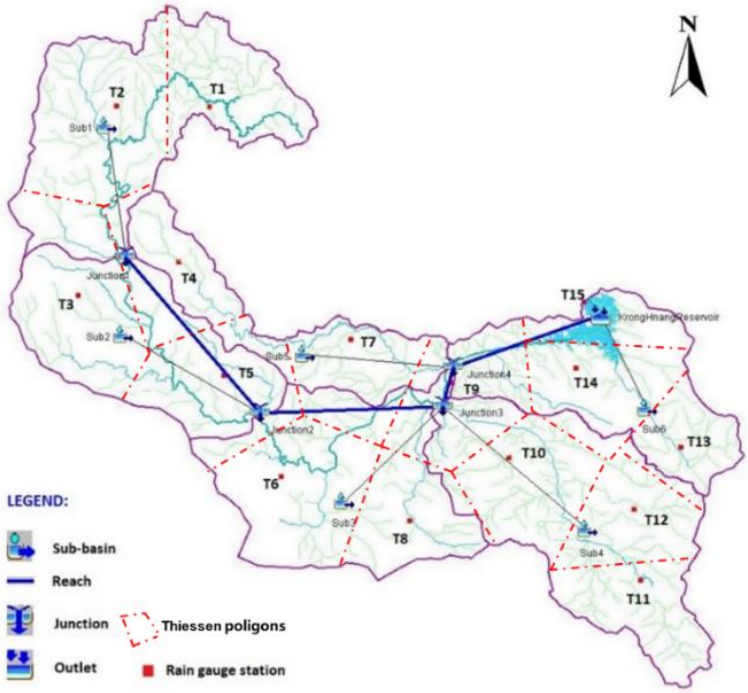

Figure 8. Representation of Krong H'nang basin in the HEC-HMS model. The basin model is compised of 6 sub-basins (Sub1 to Sub6) and four reaches (Reach-1 to Reach-4). The meteorologic component utilizes observed rainfall data from 15 sites (T1 to T15). The average rainfall on the subbasin is interpolated using the Theissen polygon method.

Table 2. Sub-basin area and length of main river sections.

Sub-basin	Sub1	Sub2	Sub3	Sub4	Sub5	Sub6
Area (km^2)	232.00	180.00	224.00	260.00	101.00	171.00
Reach	Reach1	Reach2	Reach3	Reach4		
Length (km)	25.97	25.88	2.96	15.05		

4.2. Hybrid HEC-HMS-ANN model

The number of hidden layers and the number of neurons in each hidden layer in the Encoder-Decoder LSTM network architecture are determined by trial-and-error on the training-correction dataset, loss function value. The goodness of the model is measured using the mean square error (MSE). The Google Colab platform is used for model training.

The model named 20-20-20-1, which consisting of 20 neurons on the input layer, 2 hidden layers with 20 neurons on each layer, and 1 output layer with 1 neuron, was selected as the working model. The graph of the loss function or loss function MSE (on normalized data) from the training process is shown in **Figure *9***.

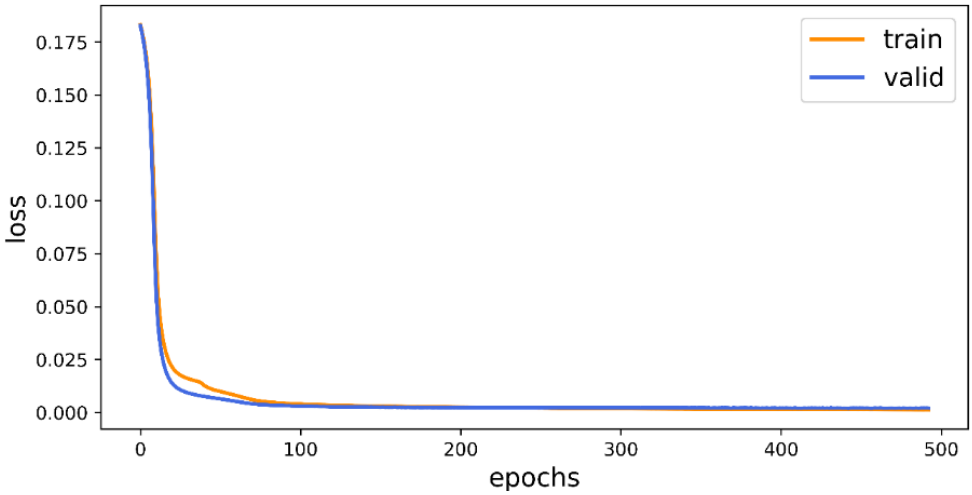

Figure 9. The loss-epochs error value of the model training process.

Figure *10* shows the hybrid model results for flood #24 at forecast time steps t+1 to t+6 hours. The increase in forecast quality in steps t + 1, t + 2 hours is minor because the HEC-HMS model and the optimal detection algorithm SCE-UA for Krong H'nang reservoir performed admirably at these time intervals. At larger forecasting time steps like t +5 and t +6 hours, the results demonstrate the hybrid model's superiority.

The model assessment criteria are summarized in **Figure *11***. The comparison between the results of the HEC-HMS model and the HEC-HMS-ANN hybrid model at the forecasting time steps $t + 1$ to $t +$ 6 hours shows that the hybrid model significantly improved the accuracy of all indicators, especially in the error of total flood volume, an important indicator in flood forecasting for reservoirs. The HEC-HMS flood peak error tends to be negative, while the hybrid model tends to be positive (ie. $Q_{sim}^{p} > Q_{obs}^{p}$), which is a safety in real-time reservoir operation.

Table 3 shows the calculation results of the hybrid model increases or decreases relative to the HEC-HMS model based on the median value compared to their ideal value by equation (16). With the synthetic evaluation index KGE, $\Delta_{KGE} =$ 16 % at the t+1 hour forecast step and up to $\Delta_{KGE} =$ 69 % at the t+6 hours step. The volume error indicator decreased slightly at step t+1 hour, $\Delta_{vol\ error} = -0{,}7$ % and then gradually increased from từ $\Delta_{vol\ error} =$ 3,5 % at step t+2 hours to $\Delta_{vol\ error} =$ 33 % at step t+6 hours. Similar to the other evaluation indices, the hybrid model shows outstanding predictive accuracy at the time steps t + 3 hours to t + 6 hours.

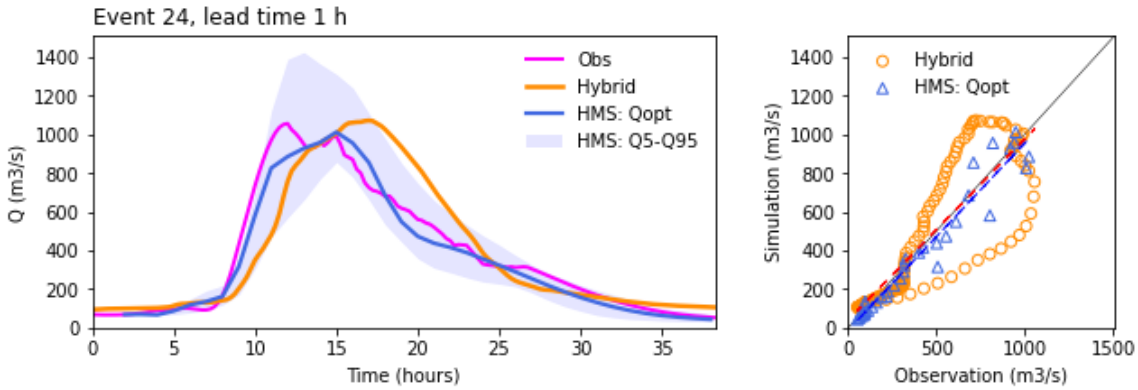

	R2	KGE	NSE	RRMSE	Peak error %	Vol error %	Tp error (hours)
HMS Model	0.946	0.929	0.939	0.203	0.16	-6.56	2.0
Hybrid Model	0.762	0.848	0.72	0.45	1.49	4.04	5.0

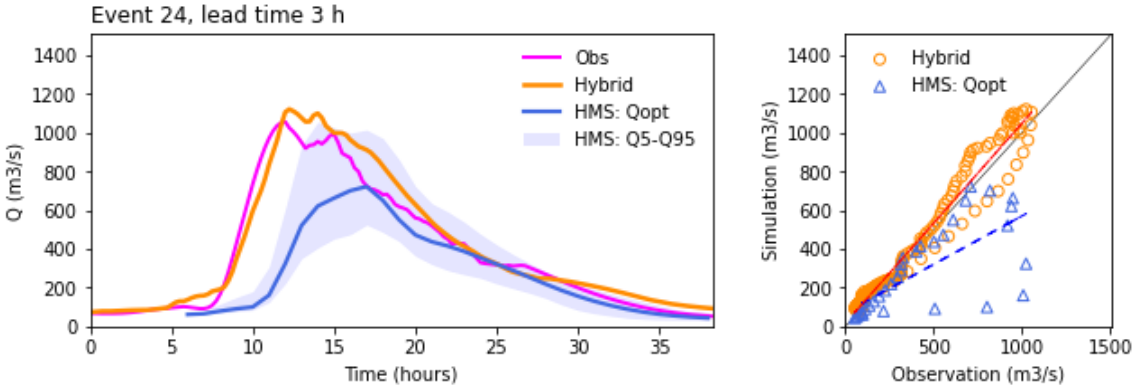

	R2	KGE	NSE	RRMSE	Peak error %	Vol error %	Tp error (hours)
HMS Model	0.517	0.471	0.343	0.636	-29.55	-32.66	5.0
Hybrid Model	0.962	0.907	0.949	0.191	6.14	7.59	0.25

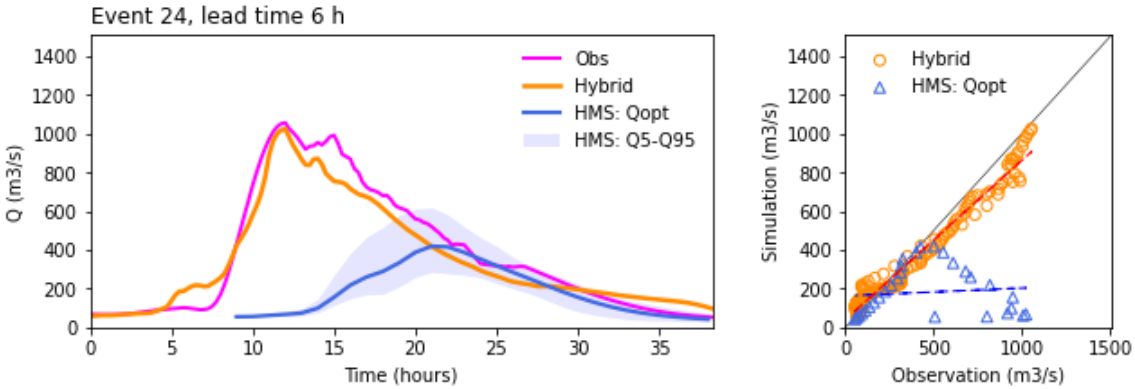

	R2	KGE	NSE	RRMSE	Peak error %	Vol error %	Tp error (hours)
HMS Model	0.01	-0.23	-0.719	0.958	-58.68	-58.6	9.0
Hybrid Model	0.968	0.819	0.939	0.211	-2.86	-7.19	0.0

Figure 10. Flood prediction results for the HEC-HMS-ANN hybrid model #24 at time steps t + 1 to t + 6 for improved forecasting quality compared to the HEC-HMS model.

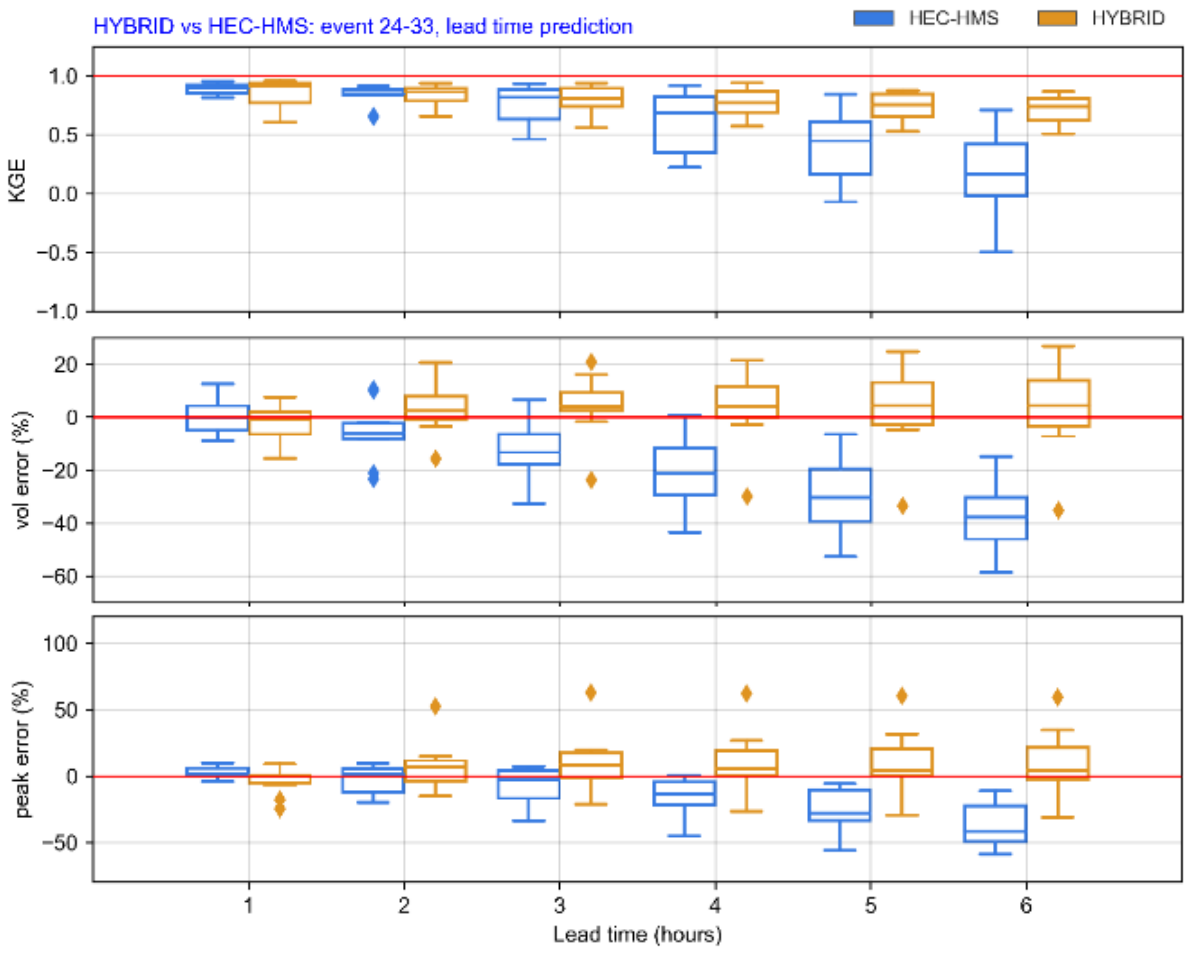

Figure 11. Summary and compare forecasting results of the HEC-HMS-ANN hybrid model and the HEC-HMS model at forecasting steps t+1 to t+6 for different evaluation criteria, including KGE, vol error (%), and flood peak error (%).

Table 3. Calculation of the increase or decrease in the goodness of the hybrid model for 10 flood events (from #24 to #33) at different time steps.

Criteria	Lead time	t +1 h	t +2 h	t +3 h	t +4 h	t +5 h	t +6 h
KGE	Best	1	1	1	1	1	1
	HEC-HMS	0,900	0,849	0,820	0,688	0,448	0,166
	Hybrid	0,916	0,865	0,809	0,773	0,753	0,740
	Δ_{KGE}	**16,0%**	**10,6%**	**-6,1%**	**27,2%**	**55,3%**	**68,8%**
Vol error %	Best	0	0	0	0	0	0
	HEC-HMS	-0,055	-5,92	-13,205	-21,25	-30,27	-37,705
	Hybrid	-0,635	2,425	4,140	4,245	4,4	4,365
	$\Delta_{vol\ error}$	**-0,7%**	**3,5%**	**9,1%**	**17,0%**	**25,9%**	**33,3%**
Peak error %	Best	0	0	0	0	0	0
	HEC-HMS	1,940	1,300	-2,805	-13,445	-28,030	-41,53
	Hybrid	-0,245	6,575	8,665	5,905	4,380	4,440
	$\Delta_{peak\ error}$	**1,7%**	**-7,9%**	**-5,9%**	**7,5%**	**23,7%**	**37,1%**

5. Conclusion

In this study, a hybrid machine-learning hydrological model based on the combination of the HEC-HMS physical model and the artificial neural network was built and tested for the Krong H'ang hydropower reservoir located in Dak Lak province, the Highlands of Vietnam. The model uses an Encoder-Decoder-Long-Short-Term-Memory Network architecture and was trained, calibrated, and tested with historical rainfall data, measured discharge, and forecasted flow from HEC-HMS at 33 flood events in the period from 2016 to 2021. The results show that the HEC-HMS-ANN hybrid model significantly improves prediction accuracy when compared to the single HEC-HMS model, especially at longer forecasting time steps, as evidenced by Δ_{KGE} = 16% at the t + 1 hour forecast step and Δ_{KGE} = 69% at the t + 6 hours forecast step. It also demonstrates that the predictive quality of the hybrid model is superior in various evaluations, such as flood peak error and flood volume error.

Because of the strong support of computer technology and large data, the hybrid machine-learning hydrological model has enhanced the accuracy of the flood prediction model, particularly over lengthy forecast periods. Forecasting ahead of time allows state management organizations, building businesses, and people to respond to changing rainfall and flood conditions.

Acknowledgments

Nguyen Phuoc Sinh was funded by Vingroup JSC and supported by the Master, PhD Scholarship Programme of Vingroup Innovation Foundation (VINIF), Institute of Big Data, code VINIF.2021.ThS.97. The authors acknowledge Song Ba Joint Stock Company to provide the database and would like to thank HEC-Support Team for their help during this study.

References

[1] Cullmann J, Dilley M, Fowler J, Grasso FV, Kabat P, Lúcio F, et al. 2020 State of climate services. WMO-No 1242 2020:1–18.

[2] NOAA. U.S. Climate Extremes Index (CEI). Climate Services and Monitoring Division 2021;2021.

[3] WMO. Decision Support for the Selection of Flood Forecasting Models. WMO Flood Forecasting Initiative 2011.

[4] WMO. Guidelines for Nowcasting Techniques. World Meteorological Organization 2017:82.

[5] Beven K. Rainfall-runoff modelling : the primer / Keith Beven. – 2nd ed. John Wiley & Sons, Ltd 2010.

[6] Chu X, Steinman A. Event and Continuous Hydrologic Modeling with HEC-HMS. Journal of Irrigation and Drainage Engineering 2009;135. https://doi.org/10.1061/(asce)0733-9437(2009)135:1(119).

[7] Martin O, Rugumayo A, Ovcharovichova J. Application of HEC-HMS / RAS and GIS Tools in Flood Modeling : A Case Study for River Sironko – Uganda. Global Journal of Engineering, Design & Technology 2012;1.

[8] Albo-Salih H, Mays LW. Real-time operation of river-reservoir systems during flood conditions using optimization/simulation with one and two-dimensional modeling. Proceedings of the International Conference on Natural Hazards and Infrastructure, 2019.

[9] Che D, Mays LW. Development of an Optimization/Simulation Model for Real-Time Flood-Control Operation of River-Reservoirs Systems. Water Resources Management 2015;29. https://doi.org/10.1007/s11269-015-1041-8.

[10] Şensoy A, Uysal G, Şorman AA. Developing a decision support framework for real-time flood management using integrated models. J Flood Risk Manag 2018;11. https://doi.org/10.1111/jfr3.12280.

[11] ASCE. Task Committee on Application of Artificial Neural Networks in Hydrology, Artificial Neural Networks in Hydrology. II:Hydrologic Application. J Hydrol Eng

2000;5.
[12] Kraft B, Jung M, Körner M, Reichstein M. HYBRID MODELING: FUSION of A DEEP LEARNING APPROACH and A PHYSICS-BASED MODEL for GLOBAL HYDROLOGICAL MODELING. International Archives of the Photogrammetry, Remote Sensing and Spatial Information Sciences - ISPRS Archives, vol. 43, 2020. https://doi.org/10.5194/isprs-archives-XLIII-B2-2020-1537-2020.
[13] ASCE. Artificial Neural Networks in Hydrology I: PRELIMINARY CONCEPTS. J Hydrol Eng 2000.
[14] Kim H Il, Han KY. Urban flood prediction using deep neural network with data augmentation. Water (Switzerland) 2020;12. https://doi.org/10.3390/w12030899.
[15] Yuan L, Forshay KJ. Enhanced streamflow prediction with SWAT using support vector regression for spatial calibration: A case study in the Illinois River watershed, U.S. PLoS One 2021;16. https://doi.org/10.1371/journal.pone.0248489.
[16] Tamiru H, Wagari M. Machine-learning and HEC-RAS integrated models for flood inundation mapping in Baro River Basin, Ethiopia. Model Earth Syst Environ 2021. https://doi.org/10.1007/s40808-021-01175-8.
[17] Gauch M, Kratzert F, Klotz D, Nearing G, Lin J, Hochreiter S. Rainfall-runoff prediction at multiple timescales with a single Long Short-Term Memory network. Hydrol Earth Syst Sci 2021;25. https://doi.org/10.5194/hess-25-2045-2021.
[18] EVN-PECC4. Krong Hnang - Technical design documents (phase 2) 2007.
[19] USACE. HEC-HMS User's Manual. US Army Corps of Engineers Hydrologic Engineering Center 2021:623.
[20] USACE. Hydrologic Modeling System HEC-HMS Technical Reference Manual. US Army Corps of Engineers 2000. https://doi.org/CDP-74B.
[21] Kratzert F, Klotz D, Brenner C, Schulz K, Herrnegger M. Rainfall-runoff modelling using Long Short-Term Memory (LSTM) networks. Hydrol Earth Syst Sci 2018;22. https://doi.org/10.5194/hess-22-6005-2018.
[22] Duan Q. and Gupta K. . Effective and efficient global optimization for conceptual rainfall-runoff models. Water Resour Res 1992;4 28.
[23] Sinh NP, Huy NT, Hung NT. Automatic calibration of HEC–HMS model using Shuffled Complex Evolution (SCE–UA) algorithm. Vietnam Journal of Hydrometeorology 2022;9:1–18. https://doi.org/10.36335/vnjhm.2022(741).1-18.